Syntrophy between fermentative and purple phototrophic bacteria to treat and valorize carbohydrate-rich wastewaters

Author(s):
Cerruti, Marta; Crosset-Perrotin, Guillaume; Ananth, Mythili; Rombouts, Julius Laurens; Weissbrodt, David G.

Publication date:
2023-06

Permanent link:
https://doi.org/10.3929/ethz-b-000671495

Originally published in:
Bioresource Technology Reports 22, https://doi.org/10.1016/j.biteb.2023.101348

Bioresource Technology Reports 22 (2023) 101348

Contents lists available at ScienceDirect

Bioresource Technology Reports

journal homepage: www.sciencedirect.com/journal/bioresource-technology-reports

Syntrophy between fermentative and purple phototrophic bacteria to treat and valorize carbohydrate-rich wastewaters

Marta Cerruti [a,*,1], Guillaume Crosset-Perrotin [a], Mythili Ananth [a], Julius Laurens Rombouts [a,b], David G. Weissbrodt [a]

[a] Department of Biotechnology, Delft University of Technology, Delft, the Netherlands
[b] Nature's Principles B.V., Den Haag, the Netherlands

ARTICLE INFO

Keywords:
Photoorganoheterotrophs
Chemoorganoheterotrophs
Syntrophy
Mixed-culture fermentation
Resource recovery

ABSTRACT

Fermentative chemoorganoheterotrophic bacteria (FCB) and purple photoorganoheterotrophic bacteria (PPB) are two interesting microbial guilds to process carbohydrate-rich wastewaters. Their metabolic interactions have been studied in pure cultures or co-cultures, but little is known about mixed cultures. We studied the effect of reactor regimes (batch/chemostat) and illumination modes (continuous infrared light, dark, or light/dark cycles) on glucose conversions and process ecology of the interactions between FCB and PPB in mixed cultures. In batch, FCB (>80 % of sequencing read counts) outcompeted PPB, under any light conditions. In chemostat under continuous and alternating irradiance, three FCB populations were enriched (>70 %), while *Rhodobacteraceae* (PPB) made 30 % of the community. Glucose fermentation products were linked to the dominant FCB. Continuous culturing helped maintaining FCB and PPB in syntrophy: PPB grew on glucose metabolites produced by FCB. Engineering the association between FCB and PPB in mixed-culture processes can help to treat and valorize carbohydrate-rich aqueous waste.

1. Introduction

In nature, microorganisms have evolved to occupy diverse functional niches (Deines et al., 2020). They form metabolic associations to grow under nutrient-limiting conditions (Pearman et al., 2008). Wastewater treatment plants (WWTPs) use microbial communities to remove relatively high concentrations of organics (up to ~60 g COD L^{-1}) (Ling et al., 2016) and other nitrogenous and phosphorous nutrients. WWTPs deal with complex compositions of organic matter like cellulose and undigested fibers from food. In agri-food industrial wastewaters, most of organics are derived from simple carbohydrates (*e.g.*, glucose, fructose or xylose) and polymeric sugars such as starch, cellulose and lignocellulosic derivates (Ghosh et al., 2017).

The wastewater treatment sector transitions to develop bioprocesses that combine nutrient removal with bioproduct valorization. Environmental biotechnologies involving mixed cultures are studied to treat and valorize nutrient-rich wastewaters by unravelling the biochemical mechanisms that can drive microbial conversions and products formations (Kleerebezem & Van Loosdrecht, 2007). The efficiency of mixed-culture processes is based on proper selection of microbial guilds needed to metabolize the wastes.

Two guilds across chemo- and photoorganoheterotrophic groups are particularly attractive to process carbohydrate- and carboxylate-rich feedstocks, namely fermentative chemoorganoheterotrophic bacteria (FCB) and purple phototrophic bacteria (PPB).

FCB like *Clostridium*, *Enterobacter*, *Lactobacillus* degrade carbohydrates through fermentation pathways, producing a spectrum of valuable compounds such as carboxylates (*e.g.*, volatile fatty acids — VFAs, lactic acid), ethanol and H_2. Their microbial niches are harnessed in non-axenic mixed-culture fermentation processes to valorize, *e.g.*, lignocellulosic sugars into targeted fermentation products like lactate or ethanol (Rombouts et al., 2019a).

Abbreviations: A_{660}, absorbance at 660 nm; μ_{max}, biomass-specific maximum growth rate; μ, biomass-specific growth rate; CSTR, continuous-flow stirred-tank reactor; FCB, fermentative chemoorganoheterotrophic bacteria; IR, infrared; PPB, purple photoorganoheterotrophic bacteria; SSQ, residual sum of squares error; SBR, sequencing batch reactor; VSS, volatile suspended solids; WWTP, wastewater treatment plants; $Y_{X/S}$, yield of biomass on substrate.

* Corresponding author at: Weissbrodt Group for Environmental Life Science Engineering, Environmental Biotechnology Section, Department of Biotechnology, TNW Building 58, van der Maasweg 9, 2629 HZ Delft, the Netherlands.
E-mail address: marta.cerruti@hest.ethz.ch (M. Cerruti).
[1] Present address: Marta Cerruti, Laboratory of Food Biotechnology, Swiss Federal Institute of Technology in Zürich, Switzerland.

https://doi.org/10.1016/j.biteb.2023.101348
Received 13 August 2022; Received in revised form 4 January 2023; Accepted 24 January 2023
Available online 1 February 2023

PPB like *Rhodobacter*, *Rhodopseudomonas*, *Rhodospirillum* are versatile microorganisms, involving a diversity of phototrophic and chemotrophic metabolisms depending on environmental and physiological conditions (Table 1). They grow preferentially as photo-organoheterotrophs, harvesting their energy from infrared (IR) light and using a variety of carbon sources from carboxylates to carbohydrates to alcohols (Puyol et al., 2017). PPB can also grow as chemotrophs using organic or inorganic substrates (Hunter et al., 2009). As photo-organoheterotrophs, they can achieve high biomass yields up to 1 g COD_X g^{-1} COD_S (Puyol et al., 2017). PPB can thus be exploited to valorize anabolic products like biomass, single-cell proteins used in animal/human feed, or industrially relevant compounds like carotenoids. PPB can also photoferment, coupling glucose degradation to H_2 production.

Combinations of fermentative, chemoorganoheterotrophy and photofermentation processes have been investigated to degrade, convert and valorize carbohydrates in different configurations using pure cultures and synthetic co-cultures of FCB and PPB. First, a two-stage process of dark fermentation and photoorganoheterotrophy has been carried in two separate reactors: in the upstream unit, a pure culture of FCB degrade carbohydrates into VFAs that are fed in the downstream unit to produce a PPB biomass in pure culture (Ghimire et al., 2015). Second, in a single-stage dark fermentation process, a pure culture of PPB has been used to convert glucose and other organics into H_2: this has necessitated longer contact times compared to the two-stage fermentation process and the requirement of a pre-sterilized feed stream and axenic environment (Abo-Hashesh & Hallenbeck, 2012). Third, in single-stage dark- and photo-fermentation process, attempts have been made to co-cultivate defined FCB and PPB to simultaneously degrade carbohydrates and convert the produced VFAs to biomass (Rai & Singh, 2016). Despite the advantages of this synthetic co-culture approach for lower investment and operation costs compared to two-stage fermentation process, it still requires an axenic environment that impacts process economics. Open mixed-culture biotechnologies associating FCB and PPB can become beneficial to treat and valorize carbohydrate-based wastewaters. Compared to traditional industrial biotechnologies, open mixed cultures do not require sterilization of the inflow and tank, therefore substantially reducing the costs (Kleerebezem & Van Loosdrecht, 2007). Based on ecological principles, microorganisms can be selected to specifically target substrate degradation, bioproduct valorization or both.

Despite the growing interest on PPB mixed cultures (reviewed elsewhere (Capson-Tojo et al., 2020)), little is known about the selection phenomena and community dynamics in open mixed cultures of FCB and PPB, and the impact of substrate composition, environmental conditions, and reactor regimes thereof. Competition and metabolic interactions between these microbial guilds have not been unraveled yet. One can also wonder whether PPB, due to their wide metabolic versatility, could be selectively enriched in a carbohydrate-fed mixed culture to complete the full network of metabolisms from glucose fermentation to photoorganoheterotrophy, or whether FCB would more efficiently ferment glucose, prior to supplying fermentation products for the PPB to grow.

Here, we evaluated the ecological association of PPB and FCB in carbohydrate-fed mixed cultures. We addressed the selection mechanisms, competitive and syntrophic interactions of the two microbial guilds across reactor regimes (batch, chemostat) and IR light irradiance patterns (continuous light, continuous dark, dark/light alternation) using either glucose or acetate as model carbohydrate and carboxylate substrates, respectively, that harbor the same degree of reduction (4 mol e^- C-mol^{-1}). With these microbial ecology insights, we tested the treatment of a carbohydrate-rich synthetic wastewater in a continuous single-stage mixed-culture process assembling FCB and PPB in syntrophy, by ecological engineering.

2. Material and methods

To evaluate microbial competition between PPB and fermenters, two mixed-culture bioreactor regimes (batch and continuous culturing), two substrates with the same degree of reduction per carbon mole (acetate and glucose), and three light patterns (continuous illumination, continuous dark, and light/dark alternation in a 16 h/8 h sequence) were applied. The reactor performances were measured by kinetic and stoichiometry endpoints (rates, yields). Microbial selection and

Table 1
Metabolic versatility of purple phototrophic bacteria (PPB). PPB can grow by combining a diversity of substrates and redox conditions. PPB grow primarily as photoorganoheterotrophs using VFAs as preferential carbon sources, but they are able to grow also on glucose with low growth rates. The metabolisms targeted in this study for the conversion of glucose by combination of fermentation and photoorganoheterotrophy are highlighted in grey.

Metabolism	Energy source (photo-/chemo-)	Electron donors (organo-/litho-)	Oxidized e-donors	Carbon source (hetero-/auto-)	Electron acceptors	Reduced e-acceptors
Under light conditions						
Anoxygenic photoorganoheterotrophy	Light photons	Reduced organic	Oxidized organic, CO_2	Organic	Endogenous compound, CO_2 fixation	Biomass
Anoxygenic photolithoautotrophy	Light photons	Reduced inorganic H_2 H_2S Fe^{2+} NO_2^-	Oxidized inorganic H_2O SO_4^{2-} Fe^{3+} NO_3^-	Inorganic (CO_2)	Endogenous compound, CO_2 fixation	Biomass
Oxygenic photolithoautotrophy	Light photons	H_2O	O_2	Inorganic (CO_2)	Endogenous compound, CO_2 fixation	Biomass
Photofermentation (not growth associated)	Light photons	Excess electrons energized from substrate	–	–	H^+	H_2
Under dark conditions						
Aerobic-respiring chemoorganoheterotrophy	Chemical redox reaction by aerobic respiration	Reduced organic	CO_2	Organic	O_2	H_2O Biomass
Anaerobic-respiring chemoorganoheterotrophy	Chemical redox reaction by anaerobic respiration	Reduced organic	CO_2	Organic	NO_3^- SO_4^{2-}	N_2 S^0, HS^-, H_2S Biomass
Fermentative chemoorganoheterotrophy	Chemical redox reaction by fermentation	Reduced organic (*e.g.*, fermentable sugars)	Pyruvate or CO_2	Organic	Endogenous compound	Fermentation products (*e.g.*, acetate, H_2), biomass

dynamics in microbial community compositions were tracked by 16S rRNA gene amplicon sequencing. The experimental design is shown in Table 2, and methods described hereafter.

2.1. Composition of cultivation media

Under all conditions, the cultures were provided with a mineral medium composed as in Cerruti et al. (2020b). The cultivation medium was buffered at pH 7.0 with 4-(2-hydroxyethyl)-1piperazineethanesulfonic acid (HEPES) at 4 g L^{-1}. Acetate and glucose were used as carbon sources, in a concentration of 5 or 10 g COD L^{-1} depending on experimental conditions (Table 2), mimicking concentrations of moderately loaded agri-food wastewaters (Oh and Logan, 2005). Acetate was provided as $C_2H_3O_2Na{\cdot}3H_2O$ (18.28 g L^{-1}) and glucose as $C_6H_{12}O_6{\cdot}H_2O$ (9.68 g L^{-1}).

2.2. Batch operational conditions

Batch tests were first operated to study the competition of PPB and FCB in discontinuous mode. PPB biomass from an in-house enrichment culture grown and maintained in a sequencing batch reactor (SBR) (Cerruti et al., 2020a) was used to inoculate 100-ml anaerobic batch bottles. The cultures were flushed with 99 % argon gas to maintain anaerobic conditions (Linde, NL, >99 % purity). Every batch bottle was duplicated. Half of the batch bottles were exposed to dark. The other half were exposed to IR light (>700 nm) supplied by a halogen lamp (white light) with a power of 120 W whose wavelengths below 700 nm were filtered out by two Black 962 Infrared Transmitting Perspex Acrylic Sheets (Black Perspex 962, Plasticstocktist, UK). Every batch was incubated in a closed shaker (Certomat® BS1, Sartorius Stedim Biotech, Germany) at 30 ± 1 °C in the dark and at 37 ± 1 °C under IR light: these temperature differences originated from the heat emitted from the lamps. The flasks were agitated at 170 rpm. The cultures were fed with 10 g COD L^{-1} of either glucose or acetate.

2.3. Continuous culturing conditions

Competition and syntrophy of FCB and PPB under continuous culturing were tested and tuned in a 2.5-L single-wall, continuous-flow stirred-tank reactor (CSTR) with a diameter of 11 cm and a working volume of 2 L, connected to a controller system (In- Control and Power units, Applikon, Netherlands). The pH was controlled at 7.0 with NaOH at 0.25 mol L^{-1} and HCl 1 mol L^{-1}. The temperature was maintained at 30 °C with a finger-type heat exchanger connected to a thermostat (WK 500, Lauda, Germany).

Similar to the batches, the reactor was irradiated from two opposite sides with two incandescent halogen lights of 120 W filtered to select for IR wavelengths $\lambda > 700$ nm using Black Perspex 962 sheets (Plasticstocktist, UK) to promote PPB growth. An effective incident light intensity of 270 W m^{-2} was measured on the reactor wall with a pyranometer (CMP3, Kipp & Zonen, The Netherlands) placed at 90° from the light source.

The reactor was inoculated with an in-house PPB enrichment, and started under batch mode. After 48 h it was switched to continuous mode. To enrich for PPB, the dilution rate was set to 0.04 h^{-1}, *i.e.*, less than half of the biomass-specific maximum growth rate (μ_{max}) of the representative PPB genus *Rhodopseudomonas* (0.15 h^{-1}) (Cerruti et al., 2020a).

Four combinations of energy patterns and carbon sources were then tested in the mixed-culture CSTR: (*i*) continuous light with acetate, (*ii*) continuous light with glucose, (*iii*) 16 h/8 h light/dark alternation cycles with acetate, and (*iv*) 16 h/8 h light/dark alternation cycles with glucose. Light/dark alternation was controlled with an automatic switch time controller (GAMMA, The Netherlands).

After 3 months of continuous cultivation, the carbon source feed was stopped, while phosphate and nitrogen sources were maintained for a period of 4 days (*ca.* 4.5 hydraulic retention times – HRTs), in order to test and confirm the hypothesis that PPB can grow on fermentation products produced by FCB.

Table 2
Combinations of operational conditions tested to address selection, competition, and interaction mechanisms between FCB and PPB.

Reactor regime	Organic substrate	Illumination	Input concentration of organic matter (g COD L^{-1})
Batch	Acetate	Continuous	10
Batch	Acetate	No (dark)	10
Batch	Glucose	Continuous	10
Batch	Glucose	No (dark)	10
CSTR	Acetate	Continuous	5/10
CSTR	Glucose	Continuous	5
CSTR	Acetate	16 h light/8 h dark	10
CSTR	Glucose	16 h light/8 h dark	10
CSTR	No carbon/ electron sources	16 h light/8 h dark	–

2.4. On-line mass spectrometry analysis of off-gas composition

The off-gas of all CSTR experiments was connected to a mass spectrometer (Thermofisher, Prima BT Benchtop MS) which was used to measure on-line the production rates of CO_2 and H_2 (used in the simulations). The full CO_2 production profile is presented in Supplementary material 1.

2.5. Sampling of mixed liquors for biomass and liquid phase analyses

All mixed liquor samples were collected in 2-mL Eppendorf tubes, centrifuged at 10,000 ×*g* for 3 min. The biomass pellet was separated from the supernatant and stored at −20 °C until further analysis. The supernatant was filtered with 0.2 μm filters (Whatman, US), and stored at −20 °C until further analysis. From the batch cultures, the samples were collected every 24 h. From the CSTR, 5 to 9 samples were collected for each condition along the experiments.

2.6. Measurement of biomass concentrations

Biomass concentrations were measured over the time course of the batch and continuous reactors by spectrophotometry (Biochrom, Libra S11, US) through absorbance at 660 nm (A_{660}). A calibration curve was established to correlate A_{660} to the concentration of volatile suspended solids (VSS): c(g VSS L^{-1}) = 0.61 A_{660} (−). The VSS concentrations were measured by taking samples from the mixed liquor, filtering them using 0.2 μm filters (Whatman, 435 USA), drying the wet filters at 105 °C in a stove for 24 h, prior to incinerating the dried filters at 550 °C in an oven for 2 h, and weighted.

2.7. Wavelength scans of biomass samples

Wavelength scan of biomass samples were done using a spectrophotometer (DR3900, Hach, Germany) to evaluate the presence of the typical PPB photopigments (carotenoids at 400–500 nm and bacteriochlorophyll at ca 850 nm). Absorbance profiles were measured at each wavelength between 320 nm and 999 nm.

2.8. Amplicon sequencing analysis of bacterial community compositions

Genomic DNA was extracted using DNeasy Powersoil microbial extraction kits (Qiagen, Hilden, Germany) accordingly to manufacturer's instructions. The DNA extracts were quantified by fluorometry (Qubit; Thermofisher, US), and stored at −20 °C (pending analysis). The

compositions of the bacterial communities of the mixed liquors were characterized from the DNA extracts by V3-V4 16S rRNA gene-based amplicon sequencing as detailed in Cerruti et al. (2020b). Aliquots of the DNA extracts were submitted to Novogene (UK) for library preparation and amplicon sequencing. The fastq files of the sequencing datasets provided from Novogene were analysed with the QIIME2 pipeline (Bolyen et al., 2019), using the Greengenes database. The sequences were deposited in the online database NCBI (n.d.) under the Bioproject code ID PRJNA759396.

2.9. Chromatography analysis of substrate conversions and fermentation products

The depletion of substrates (acetate and glucose) and the formation of fermentation products (succinate, propionate, formate, lactate, acetate, butyrate) were monitored using high-performance liquid chromatography (HPLC) (Waters, 2707, NL) equipped with an Aminex HPX-87H separation column (BioRad, USA) maintained at 60 °C. The H_3PO_4 (1.5 mmol L^{-1}) eluent was supplied at a flowrate of 0.6 mL min^{-1}. The compounds were detected by refraction index (Waters 2414, US) and UV (210 nm, Waters 2489, US). Ethanol was quantified through gas-chromatography as in Rombouts et al. (2019a, b).

2.10. Kinetic parameters

The observed yields (Y_b) in batch cultures were calculated as in Eq. 1

$$Y_b = Y_{p/s} = \frac{[P]}{[S]} \quad (1)$$

with [P] the concentration of product at the end of the batch phase and [S] the concentration of substrate at the beginning of the batch phase.

The observed yields (Y_i) in continuous cultures were calculated as in Eq. 1:

$$Y_i = Y_{p/s} = \frac{q_p}{q_s} \quad (2)$$

with q_p and q_s the biomass specific rates.

The specific biomass growth rate μ was calculated as

$$\mu = \frac{\mathrm{Ln}(X_f) - \mathrm{Ln}(X_i)}{\Delta t} \quad (3)$$

with X_f the biomass concentration at the end of the batch period, X_i the biomass concentration at the beginning of the batch period and Δt the batch phase time.

2.11. Solver for pathway utilization prediction

Based on the observed yields, a mathematical simulation was used to evaluate the contribution of the fermentative and phototrophic pathways to the carbon metabolism. The model was constructed in Microsoft Excel 16.48 minimizing the residual sum of squares (SSQ) error between modelled and measured yields:

$$min(SSQ) = min\left(\sqrt{\sum_{i=1}^{n} \frac{(\hat{y}_i - y_i)^2}{n}}\right) \quad (4)$$

where $\hat{y}_i$ is the modelled yield value and y_i is the measured yield value, and n is the amount of metabolic compounds that are considered.

The fermentation products yields (observed yields) were calculated as in Eq. 2.

The solver estimated the contribution of the singular pathways (Table 3) to the overall metabolism as fractions. The modelled yields were estimated by summing the products between the pathway fractions and their stoichiometric coefficients. The process was automatically reiterated to minimize the SSQ between the observed and the estimated

Table 3
Stoichiometric matrix of the putative reactions included in the numerical model of metabolic reactions along pathways of fermentative chemoorganoheterotrophic bacteria (FCB) and purple photoorganoheterotrophic bacteria (PPB). The reactions 1.1–1.10 were used to evaluate the contribution of each pathway under batch conditions. The reactions 1.11 and 1.13 were included in the simulation of the CSTRs.

Microbial guilds	Reactions	Pathways	Glucose	Ethanol	Acetate	Propionate	Lactate	Butyrate	Succinate	Formate	Hydrogen	Carbon dioxide	Biomass FCB	Biomass PPB	Protons	Water
			$C_6H_{12}O_6$	C_2H_6O	$C_2H_3O_2$	$C_3H_5O_2$	$C_3H_5O_3$	$C_4H_7O_2$	$C_4H_4O_4$	CH_2O_2	H_2	CO_2	$CH_{1.8}O_{0.5}$		H^+	H_2O
FCB	1.1)	Glucose → Biomass + CO_2	−1.00	0.00	0.00	0.00	0.00	0.00	0.00	0.00	−0.10	2.00	4.00	0.00	5.00	0.00
	1.2)	Glucose → Ethanol + CO_2	−1.00	2.00	0.00	0.00	0.00	0.00	0.00	0.00	0.00	2.00	0.00	0.00	0.00	0.00
	1.3)	Glucose + → Acetate + Ethanol + CO_2	−1.00	1.00	1.00	0.00	0.00	0.00	0.00	2.00	0.00	0.00	0.00	0.00	1.00	−1.00
	1.4)	Glucose → Butyrate + CO_2	−1.00	0.00	0.00	0.00	0.00	1.20	0.00	0.00	0.00	1.20	0.00	0.00	1.20	1.20
	1.5)	Glucose → Succinate	−1.00	0.00	0.00	0.00	0.00	0.00	1.71	0.00	0.00	−0.86	0.00	0.00	3.43	0.86
	1.6)	Glucose → Lactate	−1.00	0.00	0.00	0.00	2.00	0.00	0.00	0.00	0.00	0.00	0.00	0.00	2.00	0.00
	1.7)	Lactate → Acetate + Propionate + CO_2	0.00	0.00	1.00	2.00	−3.00	0.00	0.00	0.00	0.00	1.00	0.00	0.00	0.00	1.00
	1.8	Lactare + Acetate → Butyrate + CO_2	0.00	0.00	−1.00	0.00	−1.00	1.00	0.00	0.00	0.00	1.00	0.00	0.00	0.00	1.00
FCB + PPB	1.9)	Formate → CO_2 + H_2	0.00	0.00	0.00	0.00	0.00	0.00	0.00	−1.00	1.00	1.00	0.00	0.00	0.00	0.00
PPB	1.10)	Acetate → Biomass + CO_2	0.00	0.00	−1.00	0.00	0.00	0.00	0.00	0.00	−0.02	1.00	0.00	1.00	2.00	−0.38
	1.11)	CO_2 + H_2O → Biomass + H_2	0.00	0.00	0.00	0.00	0.00	0.00	0.00	0.00	0.00	−1.00	1.00	1.00	−5.00	1.60
	1.12)	Propionate → Biomass + CO_2	0.00	0.00	0.00	−1.00	0.00	0.00	0.00	0.00	0.00	2.00	0.00	1.00	8.00	2.40
	1.13)	Butyrate + Acetate → Biomass + CO_2	0.00	0.00	−1.00	0.00	0.00	−2.00	0.00	0.00	0.00	2.00	0.00	8.00	5.00	−1.20

yields through the Generalized Reduced Gradient (GRG) Nonlinear solver available in Excel. The pathways that were used in the model varied per enrichment, depending on the microbial community structure, assuming only the activity of relevant catabolic and anabolic pathways. To simulate the carbon metabolism in batch enrichments the Eqs. 1.1–1.9 were used. To simulate the pathways used in the CSTRs, Reactions 1.10–1.13 were also added (Table 3). The model output indicated, as percentage, the contribution of the individual pathways to the total carbon, oxygen, hydrogen and electrons metabolism. The flux distribution of the different pathways predicted from the model is represented a semi-quantitative way in Fig. 4. The observed and fitted yields are presented in Supplementary material 2.

3. Results & discussion

The batch and continuous reactor experiments revealed key insights into the microbial community assembly principles that govern the selection, competition and interaction of FCB and PPB in open mixed cultures in function of organic substrates, light patterns, and reactor regimes.

3.1. Selection and competition of PPB and FCB in batch cultures

3.1.1. PPB were enriched on acetate and IR light

In batches, the acetate-fed cultures grew only when subjected to light, reaching a biomass concentration of 1 g VSS L^{-1} at a biomass specific growth rate (μ) of 0.0411 ± 0.0007 h^{-1} and with a yield of biomass on substrate ($Y_{X/S}$) of 0.60 ± 0.09 C-mol_X C-mol_S^{-1}. Little growth was reported in the 6 days of cultivation for the acetate cultures in the dark (μ = 0.006 h^{-1}).

The inocula of the batches originated from a PPB in-house enrichment culture operated and maintained as SBR in parallel to the experiments. The inoculum seeded in the acetate-fed batches presented a relative abundance above 60 % (*vs.* total amplicon sequencing read counts) of the purple non-sulfur genus *Rhodopseudomonas*. In the acetate-fed batches, *Rhodopseudomonas* sp. reached as high as 80 % of the total community after 6 days of cultivation under IR light. Despite the low growth, chemoorganoheterotrophs of the family of the *Moraxellaceae* showed the highest relative abundance (80 %) in the little biomass (0.0037 ± 0.0004 g_{VSS} L^{-1}) obtained on acetate in the dark (Fig. 1A).

Acetate is one of the preferred substrates for PPB (Blankenship et al., 1995). It is assimilated into biomass by several PPB populations, through the tricarboxylic acids cycle (Pechter et al., 2016). Acetate and IR light selected for *Rhodopseudomonas* relatives of the *Xanthobacteraceae* family. Among the PPB, *Rhodopseudomonas* has the highest biomass-specific maximum growth rate (μ_{max}) on acetate (0.15 h^{-1}) (Cerruti et al., 2020a, b) and therefore was predominant at the end of the batch cultivation. The growth rate in the acetate-fed cultures in the dark was 7 times lower than under light; the biomass concentration after 6 days was 270 times lower in the dark than under light. In the dark, acetate can only be assimilated by PPB in presence of suitable electron acceptors (*e.g.*, S^0 or SO_4^{2-}) in order to produce ATP for growth by anaerobic respiration (Madigan et al., 1982). In the batches, a little amount of external electron acceptor was present in the medium (3 mmol SO_4^{2-} L^{-1}), explaining the limited growth under dark conditions.

3.1.2. FCB outcompeted PPB on glucose, independent of light supply

In the glucose-fed batches, higher biomass concentration (1 g VSS L^{-1}) and growth rate (μ of 0.070 ± 0.001 h^{-1}) were reached in the dark than in the light (0.4 g VSS L^{-1}; 0.020 ± 0.002 h^{-1}).

The inoculum of the glucose-fed batches was dominated by the purple sulfur genus *Thiobaca*, due to an unexpected variation of the microbial community composition in the parent reactor. In the glucose-based batches, the genus of *Enterobacter* was predominant (>90 %) both under light and dark (Fig. 1A).

The *Enterobacteriaceae* family is widely predominant in anaerobic environments in the presence of non-limiting concentration of monomeric carbohydrates, such as glucose (Wijffels et al., 2003). Rombouts et al. (2019a) reported an enrichment of 75 % of the genus *Enterobacter* in a glucose-fed SBR, under nutrient, temperature and pH conditions similar to the one here presented.

pH was not controlled in batch cultivations. During glucose fermentations, pH dropped to 4.0 within 48 h, despite the presence of the HEPES buffer (Fig. 1B).

3.1.3. Ethanol was the main fermentation product in glucose-fed batches

In the irradiated acetate batches, acetate was fully depleted after 6 days of incubation.

In the glucose batches, the biomass yields on glucose were 0.052 ±

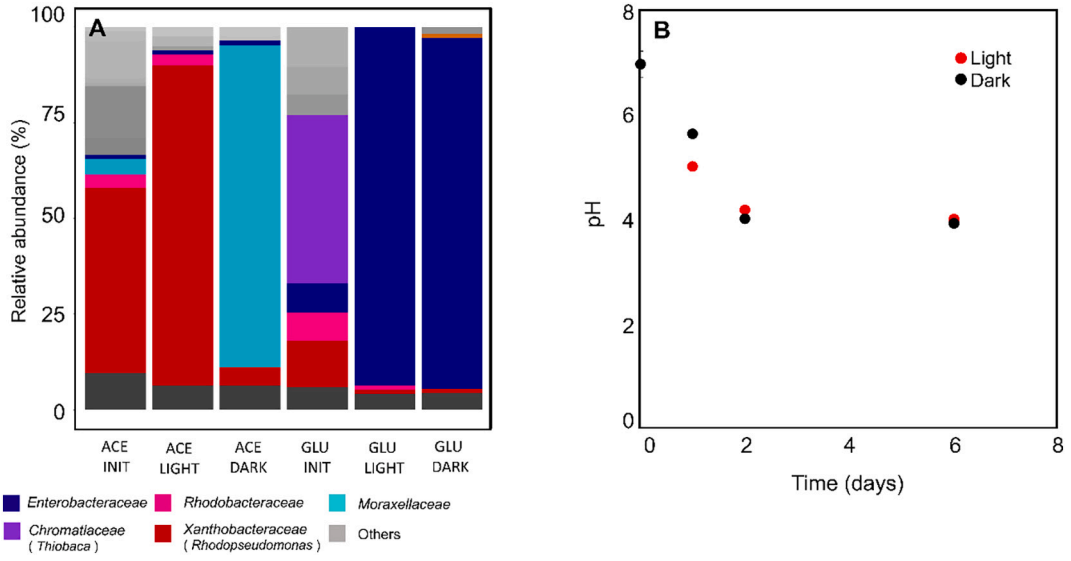

Fig. 1. A: Microbial community composition in batches. PPB are dominant at the beginning of the cultivation (ACE INIT and GLU INIT). After 6 days of cultivation under acetate feed, PPB were dominant under light conditions (ACE LIGHT). Under acetate-dark conditions there was little grow from the genus Moraxellaceae. Under glucose feed, independently of the light conditions, the family Enterobacteriaceae was dominant. B: pH evolution in the glucose-fed batches. Both under light and under dark conditions the pH dropped to 4 in the first 2 days of incubation.

0.002 C-mmol$_X$ C-mmol$_S^{-1}$ under light and 0.134 ± 0.011 C-mmol$_X$ C-mmol$_S^{-1}$ in the dark (Fig. 2).

After 6 days of dark batch fermentations of glucose, ethanol was the main fermentation product with a yield of 0.20 ± 0.10 C-mmol$_{et}$ C-mmol$_S^{-1}$, followed by succinate (0.07 ± 0.03 C-mmol$_{succ}$ C-mmol$_S^{-1}$) and acetate (0.03 ± 0.01 C-mmol$_{ace}$ C-mmol$_S^{-1}$).

In the irradiated glucose batches, 30 % of the initial glucose was still present in the reaction broth after 6 days, and carbon balances could not be properly closed (>90 % recovery). Ethanol was the main fermentation product (0.10 ± 0.07 C-mmol$_{et}$ C-mmol$_S^{-1}$), followed by lactate (0.05 C-mmol$_{lac}$ C-mmol$_S^{-1}$) and succinate (0.04 ± 0.02 C-mmol$_{succ}$ C-mmol$_S^{-1}$).

The solver enabled to evaluate the theoretical contribution of 8 putative glucose fermentation pathways to the overall carbon and electron balances. In the glucose batches, the phototrophic pathways were not included in the simulation, since the relative abundance of PPB was very low (~1 %), being outcompeted by FCB (Fig. 1A). The predicted contribution of the individual pathways to the overall yields of the batches under light and dark were comparable. In batches, the dominant metabolic pathway was identified as homo-ethanol production from glucose (Table 3, Eq. 1.2). This catabolism is associated with the fermentative *Enterobacteriaceae* (Jang et al., 2017).

Wavelength scans are commonly used as an indirect measure to rapidly check for the presence and selection of PPB in the cultures, since photopigments absorb photons with specific wavelengths. Absorbance peaks around 400–500 nm represent the carotenoids series, and the peaks around 850 nm the bacteriochlorophyll a (bchl a) (Stomp et al., 2007). In the acetate-based irradiated batches, the aforementioned peaks were clearly detected at 450 nm for carotenoids and 800–850 nm for bchl a. In the acetate-fed dark batches, almost no growth was reported within the 6 days of incubation but peak for photopigments was detected at 800 and 850 nm. No photopigment characteristic peaks were detected in the spectra of the biomasses cultivated in both the dark and irradiated glucose-fed batches, (Fig. 3A/B).

Overall, in anaerobic batches, PPB are predominantly selected with acetate and IR light. FCB outcompete PPB on glucose independent of light or dark conditions.

3.1.4. *Enterobacteriaceae were enriched due to higher growth rates*

In batch, μ_{max} is a key factor driving selection mechanisms in substrate-rich environments (Kuenen, 2019; Winkler et al., 2017), if no significant intermediate storage of substrate is displayed. FCB populations of the genus *Enterobacter* present a μ_{max} of 0.45–0.80 h^{-1} in mineral medium conditions with moderate sugar concentrations (<10 g$_{COD}$ L^{-1}) (Rombouts et al., 2019a). When fermenting carbohydrates like glucose in pure culture, *Rhodopseudomonas capsulata* grows at a μ_{max} of 0.014 h^{-1} (Conrad and Schlegel, 1978). In batches, where the substrate is not limiting across most of the conversion time, the organisms with higher substrate uptakes rates get selected above organisms with high biomass yields (Rombouts et al., 2019a, b). According to the

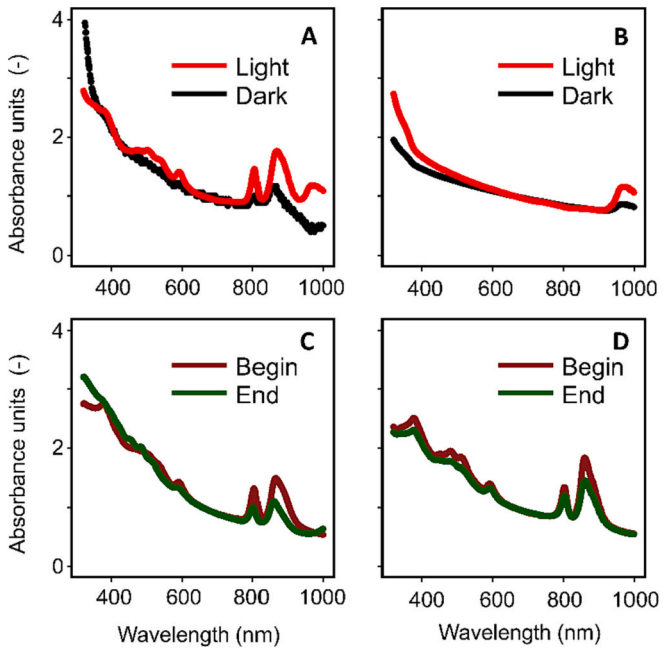

Fig. 3. Wavelength scan from 300 to 1000 nm. Absorbance units normalized for the biomass concentration (as A.U. at 660 nm). A: acetate-fed batches. The typical PPB peaks (at ca 850 nm) were clearly visible under light conditions. B: glucose-fed batches. No peak was present. C: continuous light glucose-fed CSTR. The presence of PPB was confirmed by the presence of their typical peaks. D: dark/light glucose-fed CSTR. The presence of PPB was confirmed by the presence of their typical peaks.

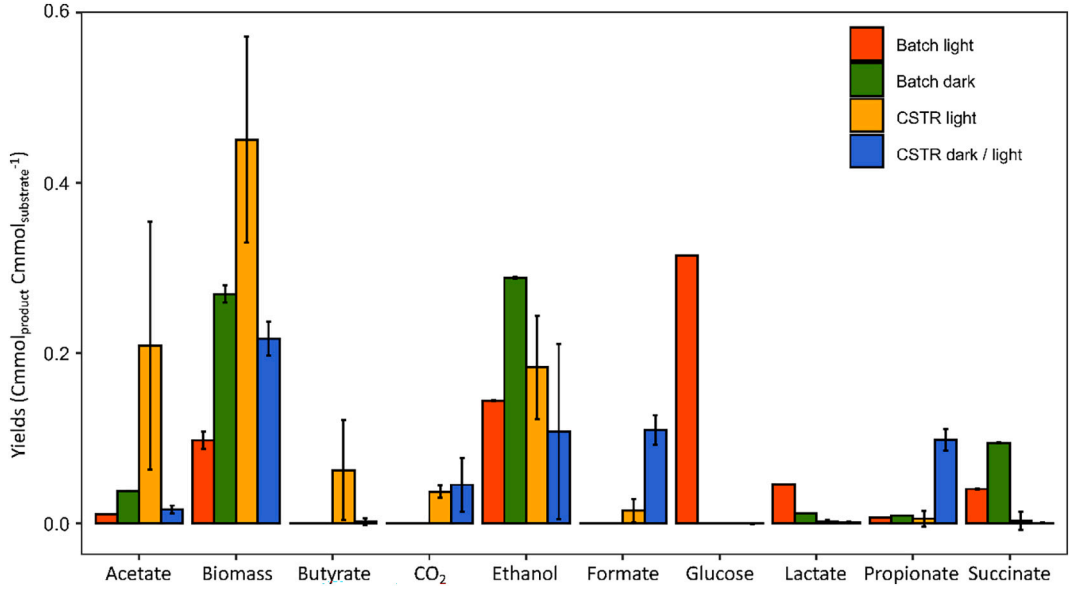

Fig. 2. Yields of the glucose-fed cultures. Under batch conditions, the main fermentation products were ethanol and succinate. Under light conditions, glucose was not fully depleted. Under CSTR conditions, the main fermentation products were ethanol, formate and acetate.

Herbert-Pirt relation, when the substrate uptake is directly coupled with growth, the organisms with the highest growth rate dominate. Using these studies, the genus *Enterobacter* is estimated to exhibit a μ_{max} about 32 times higher than *Rhodopseudomonas* on glucose, making FCB successful to outcompete PPB for glucose in batch.

In both irradiated and dark batches fed with glucose, populations of the family of *Enterobacteriaceae* were enriched (>90 %). *Enterobacteriaceae* relatives ferment sugars through either the Embden-Meyerhof pathway or the pentose phosphate pathway, with a net production of ethanol (Jang et al., 2017). Ethanol can be used as substrate for growth by PPB, but with a strict pH regulation at 7.0 (Inui et al., 1995). Because of the production of lactate (pKa = 3.8) – a major byproduct of the glucose fermentation pathway to ethanol (Converti and Perego, 2002) – and insufficient pH buffering, the pH dropped to 4.0 within the first 2 days of glucose fermentation (Fig. 1B). FCB can still grow at low pH such as below 5.5 (Tsuji et al., 1982). PPB grow instead in a pH range between 6.5 and 9.0, with an optimum at 7.0 (Pfennig, 1977). The low pH (pH = 4.0) resulting in the glucose-fed batches may have prevented PPB to grow on alcohols and VFAs produced by *Enterobacter*, explaining their low relative abundance (~1 %). We postulate that with a strict pH control of the batch cultures to 7.0, PPB should be able to grow on fermentation products of FCB.

The genus *Enterobacter* can grow in a range of temperatures between 20 and 45 °C (Gill and Suisted, 1978), with an optimum growth at 40 °C (Tanisho, 1998). The temperature differences reported here for the batches incubated under dark (30 °C) and light (37 °C) (*i.e., ca.* 7 °C difference, resulting from the heat emitted by the lamps) should not have substantially affected its specific growth rates. On the other hand, light irradiance has been used as a method to prevent the proliferation of fermentative organisms (de Sousa et al., 2016; Gwynne and Gallagher, 2018; Han et al., 2020).Since the illuminated cultures were supplied with IR light, although less energetic than white light, we postulate an inhibitory action on FCB, possibly explaining the 3.5-times lower growth rates measured under light than in the dark. The effective inhibition mode of action of photons on cellular and molecular level remains to be elucidated by future works.

3.2. *Unravelling the selection and syntrophy of FCB and PPB in continuous cultures*

Under continuous-flow regime, four different light and substrate conditions were imposed, namely: i) acetate under light; ii) acetate under dark/light cycles; iii) glucose under light; and iv) glucose under dark/light cycles. The pH was controlled at 7.0 to favor the enrichment of PPB.

3.2.1. *Ethanol was the main fermentation product*

In glucose-fed CSTRs, the biomass yield over glucose was 0.22 ±

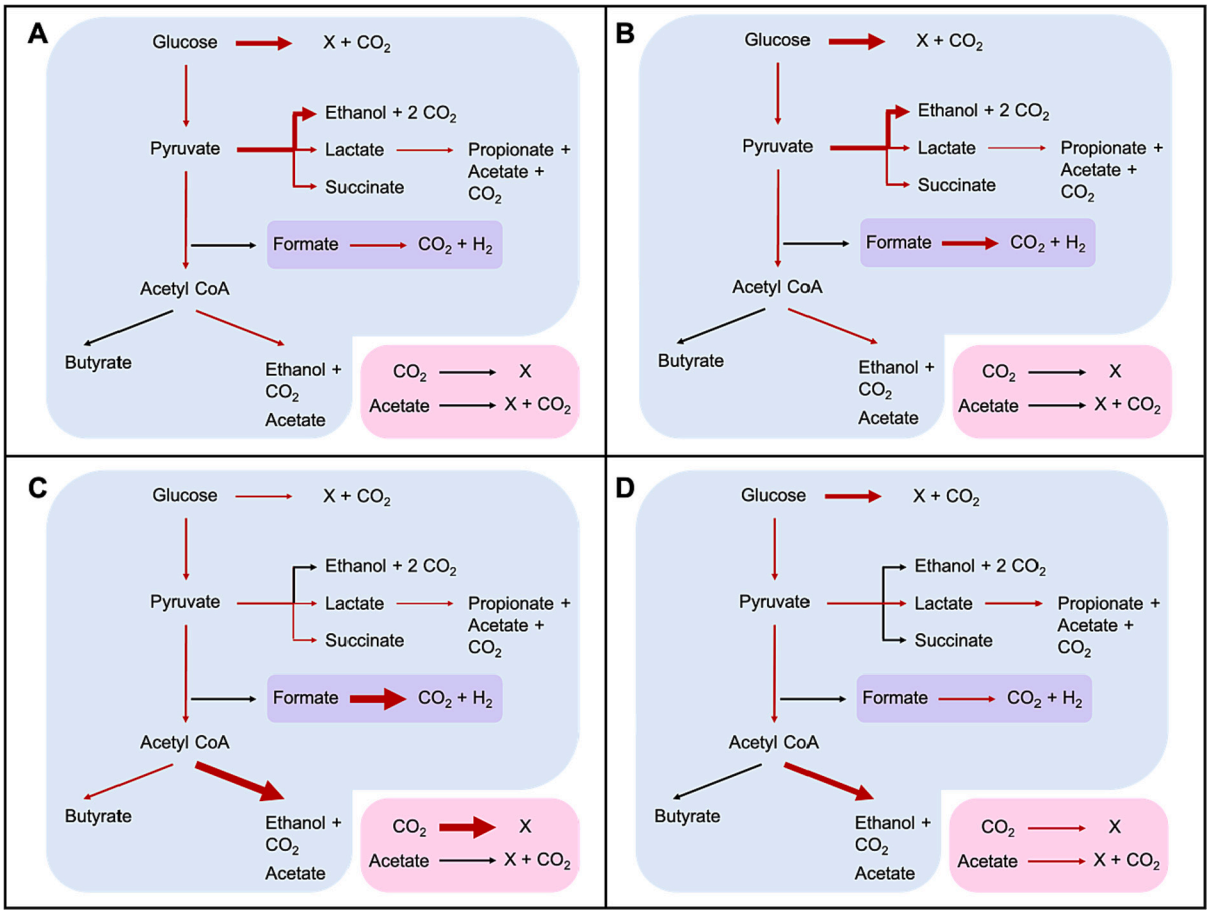

Fig. 4. Pathways involved under the different reactor regimes. The thickness of the arrows represents the predicted yield toward a specific metabolic route, based on the calculations of the solver. The reactions with the blue background are performed by FCB. The reaction with the purple background is performed by both FCB and PPB. The reactions with the pink background are performed by PPB. A: batch conditions with continuous illumination. B: batch conditions in the dark. C: CSTR under continuous illumination. D: CSTR conditions under light/dark cycles. Under batch conditions the pathways used were mainly directed toward biomass and ethanol production. Under CSTR ethanol was the main fermentation product, but the production of propionate, succinate and lactate was predicted. The phototrophic pathways were not included for the batch conditions but were included in the carbon and electron balance of the CSTRs. The conversions number 1.10, 1.12 and 1.13 of Table 3 were not included in the diagram as the solver predicted 0 % flux through them under all conditions. (For interpretation of the references to colour in this figure legend, the reader is referred to the web version of this article.)

0.02 C-mmol$_X$ C-mmol$_S^{-1}$ under continuous illumination and 0.45 ± 0.12 C-mmol$_X$ C-mmol$_S^{-1}$ under dark/light cycles. Ethanol was the main fermentation product (0.18 ± 0.06 under continuous light and 0.11 ± 0.10C-mmol$_{et}$ C-mmol$_S^{-1}$ under dark/light cycles). In the continuously irradiated CSTR, acetate (0.21 ± 0.15C-mmol$_{ace}$ C-mmol$_S^{-1}$) and butyrate (0.06 ± 0.05C-mmol$_{but}$ C-mmol$_S^{-1}$) were also produced. In the dark/light CSTR, formate (0.11 ± 0.01C-mmol$_{form}$ C-mmol$_S^{-1}$) and butyrate (0.10 ± 0.01C-mmol$_{but}$ C-mmol$_S^{-1}$) were present in the fermentation product spectrum (Fig. 2).

In CSTR, assimilation of acetate by photoorganoheterotrophy and CO_2 fixation (photosynthesis) by photolithoautotrophy were added to the solver matrix to evaluate the contribution of PPB to the total carbon and electron balances. Under all CSTR conditions, the major fermentation pathway involved fermentation of glucose through acetyl-CoA (Fig. 4), up to 83 % under continuous illumination and 55 % under dark/light cycles. In the continuously irradiated CSTR, the solver estimated a high contribution of the carbon fixation pathway enabling PPB to recycle CO_2 as extra carbon source, and of the photo-organoheterotrophic pathway under dark/light cycles.

3.2.2. PPB were enriched in the acetate-fed CSTR

In the continuously illuminated CSTR fed with acetate, PPB formed the dominant guild (68 ± 21 %) (Fig. 5). The genus *Rhodopseudomonas* was predominant at the beginning of the CSTR (65 %). Its relative abundance decreased to 40 % after one week of cultivation (8.5 HRTs), while the genus *Rhodobacter* got concomitantly enriched (from 13 to 23 %). *Rhodobacter* was further enriched once the dark/light cycles were applied, reaching 65 % after 15.6 HRTs, while *Rhodopseudomonas* remained stable below 10 %.

3.2.3. FCB were enriched in the glucose-fed CSTR

In the CSTR, the relative abundance of FCB was above 50 % under glucose feed, regardless of the light condition. In CSTR, dark/light cycles impacted the selection of FCB. Under continuous illumination, the family of *Lachnospiraceae* was predominant (around 30 %, with a peak at 75 %), followed by the family of *Enterobacteriaceae* (15 %) (Fig. 5). Under dark/light cycles, *Enterobacteriaceae* (32 ± 17 %) and *Clostridiaceae* (18 ± 15 %) relatives were predominant.

Rhodobacter was the only PPB to significantly persist in the glucose-fed CSTR (19.5 ± 14 %) (Fig. 5) independently of the illumination regime. The persistence of PPB in the glucose-fed CSTRs was further proven by the wavelength scan. Peaks for carotenoids (400–450 nm) and bacteriochlorphyll a (800 and 850 nm) photopigments were identified for both the continuous illumination and dark/light cycles (Fig. 3C/D).

3.2.4. The microbial composition of the fermentative guild defined the spectrum of fermentation products

Clostridiaceae, *Enterobacteri*aceae and *Lachnospiraceae* relatives are all able to ferment glucose. They compete for glucose through different fermentation pathways (Grimmler et al., 2011; Horiuchi et al., 2002). *Lachnospiraceae* and *Clostridiaceae* are phylogenetically and morphologically heterogeneous families belonging to the phylum of *Firmicutes* (Vos et al., 2005). Glucose fermentation through acetyl-CoA is typical of *Clostridiaceae* (Aristilde et al., 2015). In human gut microbiota, they contribute to sugar fermentation to lactate and short-chain fatty acids production (Venegas et al., 2019). Butyrate was produced only in the CSTR under continuous illumination (0.06 ± 0.05 C-mmol C-mmol$_S^{-1}$). The *Lachnospiraceae* and *Clostridiaceae* families ferment glucose into primarily butyrate, acetate and ethanol (Rombouts et al., 2019b; Temudo et al., 2008). Butyrate is produced through the butyryl-CoA dehydrogenase gene, responsible for the conversion of crotonyl-CoA to butyryl-CoA and the butyryl-CoA:acetyl-CoA transferase (Venegas et al., 2019). According to the NCBI database (NCBI), the gene encoding for this enzyme is present in the phylum of *Firmicutes* that comprises *Clostridiaceae* and *Lachnospiraceae* relatives, but not in the proteobacterial family of the *Enterobacteriaceae*, explaining the absence of butyrate in the glucose-fed batches.

In the dark/light CSTR, the relatively high production of propionate (0.10 ± 0.01 C-mmol C-mmol$_S^{-1}$, *i.e.*, 17 times higher than under continuous illumination) can be linked to the abundance of *Clostridiaceae*, which are propionate producers (Johns, 1952). *Clostridium* species can present a μ_{max} of 0.25 h^{-1} (Gomez-Flores et al., 2015) with primary fermentation products including ethanol, butyrate, acetate and propionate (Lamed et al., 1988). *Clostridium beijerincki* decreases its H_2 production when exposed to light intensities above 200 W m^{-2}, with a shift from a preferential production of butyric acid to acetic acid

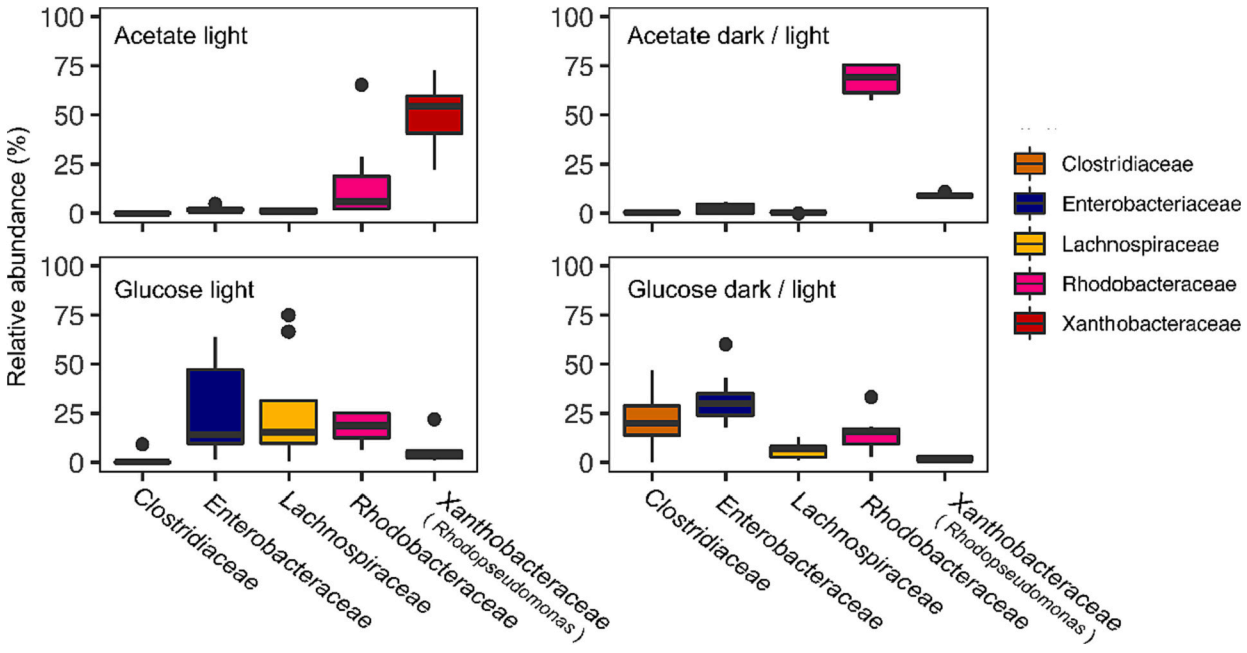

Fig. 5. Relative abundance of five representative families under CSTR conditions based on 16 s rRNA gene amplicon sequencing analysis. Under acetate conditions, PPB were dominant community, with a shift from *Rhodopseudomonas* under continuous illumination to *Rhodobacter* under light/dark conditions. Under glucose feed, the FCB were dominant, especially the genera Enterobacteriaceae and *Lachnospiraceae*.

(Zagrodnik and Laniecki, 2016). Continuous illumination in the CSTR might have inhibited *Clostridiaceae* and selected for other *Firmicutes* like *Lachnospiraceae*.

Formate and propionate production was 10 times higher under dark/light conditions compared to continuous illumination. Acetate production was instead 12 times lower under dark/light cycles compared to continuous illumination (Fig. 2). This may link to a higher relative abundance of *Enterobacteriaceae* relatives under dark/light cycles (31 %) compared to the continuous illumination (18 %) (Fig. 5). *Enterobacteriaceae* present a μ_{max} between 0.5 and 1 h^{-1} (Khanna et al., 2012; Martens et al., 1999) and are known to ferment sugars to primarily ethanol, with lactate and acetate as major byproducts (Converti and Perego, 2002).

3.2.5. *PPB metabolized the fermentation products released by FCB*

After 3 months of CSTR operation, we tested the hypothesis that PPB grow on the fermentation products of FCB. Glucose supply in the feed was stopped while nitrogen and phosphate were still provided over 4 days (*i.e.*, 4.5 HRTs). Along the 4 days of operation, the relative abundance of the PPB shifted from 10 to 50 % (Fig. 6A). The biomass concentration sharply decreased already 2 h after stopping the glucose feed, from 80 C-$mmol_X$ L^{-1} and stabilizing at a concentration of 15.7 ± 2 C-$mmol_X$ L^{-1}. Butyrate, ethanol, formate, lactate, propionate and succinate were washed out of the system at the imposed dilution rate (0.04 h^{-1}). Acetate was depleted in 50 h, *i.e.*, 4 times faster than the theoretical washout rate (Fig. 6B). In absence of glucose as carbon source, the highly active fermentative organisms were not growing. The increase in the PPB relative abundance proved their interaction with FCB, showing that PPB utilize VFAs and in particular acetate as preferred substrate and can selectively grow on FCB fermentation products.

3.3. *Metabolic strategies for tuning the microbial assembly of FCB and PPB*

Microorganisms use a combination of adaptive reactions to coexist with other organisms. Based on the adaptation techniques, two major types of organisms can be identified (Andrews and Harris, 1986), namely r- and K-strategists. The r-strategists show high growth and conversion rates, in low-populated and resources-rich environments. K-strategists thrive in highly populated environments, where the resources are limited. They exhibit lower growth rates but high substrate conversion yields.

Under the different reactor regimes, the microbial communities followed this postulate. *Enterobacteriaceae* were predominant under non-limiting conditions (batches) and can be classified as r-organisms. *Clostridiaceae* and *Lachnospiraceae* showed high growth rates in nutrient-limiting environments (chemostat) and can be classified as K-strategists. Among the PPB guild, *Xanthobacteraceae* like *Rhodopseuodmonas* showed a high-rate behavior, dominating in substrate-rich environments. *Rhodobacteraceae* showed high efficiency typical of K-organisms, being able to survive to nutrient-limited environments, as the CSTRs (Table 4). A predominance of the *Rhodopseudomonas* genus over *Rhodobacter* genus was also reported in other nutrient-rich environments (Allegue et al., 2022; Cerruti et al., 2020a, b).

Kinetic parameters define the microbial selection mechanisms in CSTRs (Kuenen, 2019). In the CSTRs, the dilution rate set to retain PPB in the system was relatively low (0.04 h^{-1}) compared to the maximum growth rates of the fermentative organisms (0.5–1 h^{-1}). In a continuous culture, the substrate (here glucose) is the limiting compound, and the organisms with higher affinity for it dominate (Andrews and Harris, 1986). Within the guild of FCB, *Clostridiaceae* and *Lachnospiaraceae* are expected to harbor a lower affinity constant (K_s), outcompeting *Enterobacteriaceae*. The controlled pH (7.0) and appropriate dilution rate (0.04 h^{-1}) sustained the persistence of PPB. Notably, *Rhodobacteraceae* were enriched in the glucose-fed CSTRs regardless the illumination conditions. We propose here a syntrophic association of FCB and PPB for glucose conversion toward CO_2 and biomass (Fig. 4). Glucose was first converted into acetate, ethanol, formate and lactate, and lactate was further transformed into acetate and propionate. All the fermentation products can be potentially used by PPB for growth. Our results, however, showed that the preferred substrate for PPB was acetate.

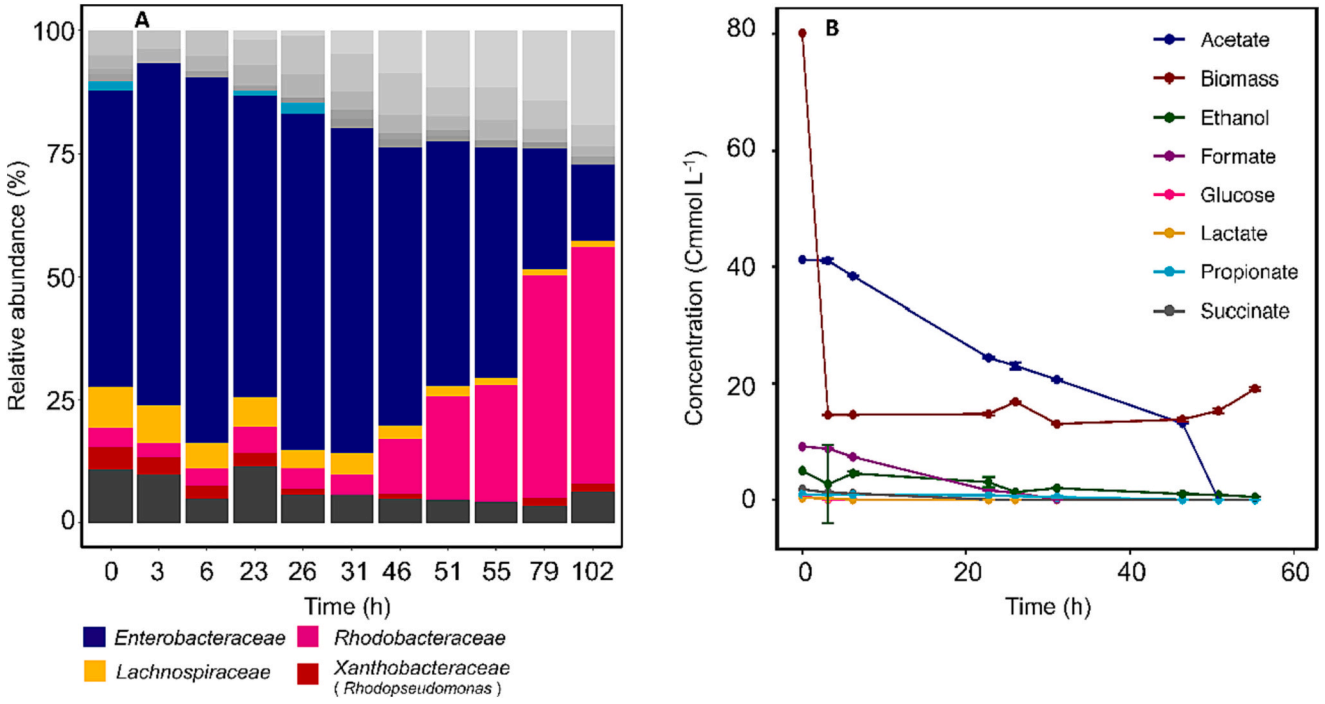

Fig. 6. A: Microbial composition after the stop to the glucose feed in the CSTR. Over time, the FCB relative abundance decreased over time, while the *Rhodobacteraceae* increased. B: Fermentation products concentration after the glucose feed-stop. After 55 h all the fermentation products were depleted.

Table 4
Reported maximum growth rates of the main FCB and PPB in the systems under glucose and acetate feed and adaptation strategies.

Substrates	Maximum growth rate μ_{max} (h^{-1})				
	Fermentative chemoorganoheterotrophic bacteria (FCB)			Purple photoorganoheterotrophic bacteria (PPB)	
	Enterobacteriaceae	*Lachnospiraceae*	*Clostridiaceae*	*Rhodopseudomonas*	*Rhodobacter*
Glucose	0.3–1 (Hasona et al., 2004; Khanna et al., 2012)	0.3 (Soto-Martin et al., 2020)	0.25 (Gomez-Flores et al., 2015)	0.014 (Conrad and Schlegel, 1978)	0.1 (Imam et al., 2011)
Acetate	–	–	–	0.15 (Cerruti et al., 2020a, b)	0.05 (Kopf and Newman, 2012)
Selection strategy	r-Strategist (on glucose)	K-strategist (on glucose)	K-strategist (on glucose)	r-Strategist (on acetate)	K-strategist (on acetate)

3.3.1. *Advantages of single-sludge and two-sludge processes for the treatment and valorization of carbohydrate-based aqueous feedstocks by FCB and PPB*

The single-step bioprocess implemented here by combining the metabolisms of FCB and PPB in one single sludge can help to simultaneously treat carbohydrate-rich wastewaters, factually removing the organic pollutants, and enriching organisms with high industrial potential (*i.e.* for single cell proteins and photopigments production). An integrated single-stage process combining fermentation and photo-organoheterotrophy allows to treat carbohydrates in only one tank, therefore minimizing capital and operating expenditures. The illumination conditions did not affect the syntrophy between FCB and PPB. A discontinuous illumination can further reduce the operational costs compared to a continuously irradiated system (Qin et al., 2018). Understanding interactions between the FCB and PPB will help design efficient processes for carbohydrates-based wastewater treatment and valorization, for instance toward the production of single cell proteins. If the aim is to maximize and valorize the PPB biomass, a two-sludge process can be efficient to first ferment carbohydrates in a first tank selecting for FCB and supply the fermentation products (whose spectrum can be engineered by mastering the selection of fermentative microbial niches) to a subsequent photoorganoheterotrophic compartment to select for, *e.g.*, an edible PPB biomass, both tanks being operated as selective open mixed cultures.

4. Conclusions

We elucidated the competitive and syntrophic phenomena between FCB and PPB using a mixed culture approach. FCB degraded glucose into VFAs, lactate and ethanol, used by PPB for growth. Operational conditions were crucial to establish interactions between FCB and PPB. In glucose-fed batches, FCB outcompeted PPB due to faster growth rate and pH drop. In glucose-fed CSTRs PPB got enriched up to 30 % in syntrophic association with FCB while pH was regulated at 7.0. The evaluation of reactor regimes and light patterns effect is crucial to establish an efficient syntrophy between PPB and FCB for carbohydrate-rich water treatment.

CRediT authorship contribution statement

MC: conceptualization, experimental research, data curation, writing; GCP: experimental research, data curation; MA: experimental research; JLR: formal analysis; DGW: review and editing, supervision, funding acquisition.

Declaration of competing interest

The authors declare that the research was conducted in the absence of any commercial or financial relationships that could be construed as a potential conflict of interest.

Data availability

The dataset related to this article can be found at the URL https://www.ncbi.nlm.nih.gov/bioproject/PRJNA759396, hosted by the NCBI database.

Acknowledgement

This study was financed by the tenure-track start-up grant of the Department of Biotechnology of the Faculty of Applied Sciences of the TU Delft (DW, PI).

Appendix A. Supplementary data

Supplementary data to this article can be found online at https://doi.org/10.1016/j.biteb.2023.101348.

References

Abo-Hashesh, M., Hallenbeck, P.C., 2012. Microaerobic dark fermentative hydrogen production by the photosynthetic bacterium, Rhodobacter capsulatus JP91. International Journal of Low-Carbon Technologies 7 (2), 97–103. https://doi.org/10.1093/ijlct/cts011.

Allegue, L.D., Ventura, M., Melero, J.A., Puyol, D., 2022. Unraveling PHA production from urban organic waste with purple phototrophic bacteria via organic overload. Renew. Sust. Energ. Rev. 166, 112687 https://doi.org/10.1016/J.RSER.2022.112687.

Andrews, J.H., Harris, R.F., 1986. In: r- and K-Selection and Microbial Ecology, pp. 99–147. https://doi.org/10.1007/978-1-4757-0611-6_3.

Aristilde, L., Lewis, I.A., Park, J.O., Rabinowitz, J.D., 2015. Hierarchy in pentose sugar metabolism in Clostridium acetobutylicum. Appl. Environ. Microbiol. 81 (4), 1452–1462. https://doi.org/10.1128/AEM.03199-14.

Blankenship, R., Madigan, M., Bauer, C., 1995. In: Blankenship, R.E., Madigan, M.T., Bauer, C.E. (Eds.), Anoxygenic Photosynthetic Bacteria, 2. Springer, Netherlands. https://doi.org/10.1007/0-306-47954-0.

Bolyen, E., Rideout, J.R., Dillon, M.R., Bokulich, N.A., Abnet, C.C., Al-Ghalith, G.A., Alexander, H., Alm, E.J., Arumugam, M., Asnicar, F., Bai, Y., Bisanz, J.E., Bittinger, K., Brejnrod, A., Brislawn, C.J., Brown, C.T., Callahan, B.J., Caraballo-Rodríguez, A.M., Chase, J., Caporaso, J.G., 2019. Reproducible, interactive, scalable and extensible microbiome data science using QIIME 2. Nature Biotechnology 37 (8), 852–857. https://doi.org/10.1038/s41587-019-0209-9.

Capson-Tojo, G., Batstone, D.J., Grassino, M., Vlaeminck, S.E., Puyol, D., Verstraete, W., Kleerebezem, R., Oehmen, A., Ghimire, A., Pikaar, I., Lema, J.M., Hülsen, T., 2020. Purple phototrophic bacteria for resource recovery: challenges and opportunities. Biotechnol. Adv. 43 (March), 107567 https://doi.org/10.1016/j.biotechadv.2020.107567.

Cerruti, M., Ouboter, H.T., Chasna, V., van Loosdrecht, M.C.M., Picioreanu, C., Weissbrodt, D.G., 2020. Effects of light/dark diel cycles on the photoorganoheterotrophic metabolism of Rhodopseudomonas palustris for differential electron allocation to PHAs and H2. BioRxiv. https://doi.org/10.1101/2020.08.19.258533.

Cerruti, M., Stevens, B., Ebrahimi, S., Alloul, A., Vlaeminck, S.E., Weissbrodt, D.G., 2020. Enrichment and aggregation of purple non-sulfur bacteria in a mixed-culture sequencing-batch photobioreactor for biological nutrient removal from wastewater. Front. Bioeng. Biotechnol. 8 https://doi.org/10.3389/fbioe.2020.557234.

Conrad, R., Schlegel, H.G., 1978. Regulation of Glucose, Fructose and Sucrose Catabolism in Rhodopseudomonas capsulata. J. Gen. Microbiol. 105 (2), 315–322. https://doi.org/10.1099/00221287-105-2-315.

Converti, A., Perego, P., 2002. Use of carbon and energy balances in the study of the anaerobic metabolism of Enterobacter aerogenes at variable starting glucose concentrations. Appl. Microbiol. Biotechnol. 59 (2–3), 303–309. https://doi.org/10.1007/s00253-002-1009-5.

de Sousa, N.T.A., Gomes, R.C., Santos, M.F., Brandino, H.E., Martinez, R., de Jesus Guirro, R.R., 2016. Red and infrared laser therapy inhibits in vitro growth of major

bacterial species that commonly colonize skin ulcers. Lasers Med. Sci. 31 (3), 549–556. https://doi.org/10.1007/S10103-016-1907-X/FIGURES/3.
Deines, P., Hammerschmidt, K., Bosch, T.C.G., 2020. Exploring the Niche Concept in a Simple Metaorganism. Front. Microbiol. 11. https://doi.org/10.3389/fmicb.2020.01942.
Ghimire, A., Frunzo, L., Pirozzi, F., Trably, E., Escudie, R., Lens, P.N.L., Esposito, G., 2015. A review on dark fermentative biohydrogen production from organic biomass: Process parameters and use of by-products. Applied Energy 144, 73–95. https://doi.org/10.1016/j.apenergy.2015.01.045.
Ghosh, S., Dairkee, U.K., Chowdhury, R., Bhattacharya, P., 2017. Hydrogen from food processing wastes via photofermentation using Purple Non-sulfur Bacteria (PNSB) – A review. Energy Convers. Manag. 141, 299–314. https://doi.org/10.1016/j.enconman.2016.09.001.
Gill, C.O., Suisted, J.R., 1978. The effects of temperature and growth rate on the proportion of unsaturated fatty acids in bacterial lipids. J. Gen. Microbiol. 104 (1), 31–36. https://doi.org/10.1099/00221287-104-1-31.
Gomez-Flores, M., Nakhla, G., Hafez, H., 2015. Microbial kinetics of Clostridium termitidis on cellobiose and glucose for biohydrogen production. Biotechnol. Lett. 37 (10), 1965–1971. https://doi.org/10.1007/s10529-015-1891-4.
Grimmler, C., Janssen, H., Krauße, D., Fischer, R.J., Bahl, H., Dürre, P., Liebl, W., Ehrenreich, A., 2011. Genome-wide gene expression analysis of the switch between acidogenesis and solventogenesis in continuous cultures of Clostridium acetobutylicum. J. Mol. Microbiol. Biotechnol. 20 (1), 1–15. https://doi.org/10.1159/000320973.
Gwynne, P.J., Gallagher, M.P., 2018. Light as a broad-spectrum antimicrobial. Front. Microbiol. 9 (FEB) https://doi.org/10.3389/fmicb.2018.00119.
Han, Q., Lau, W., Do, T.C., Zhang, Z., Xing, B., 2020. Near-infrared light brightens bacterial disinfection: recent progress and perspectives. ACS Appl. Bio Mater. 2021, 3961. https://doi.org/10.1021/acsabm.0c01341.
Hasona, A., Kim, Y., Healy, F.G., Ingram, L.O., Shanmugam, K.T., 2004. Pyruvate Formate Lyase and Acetate Kinase are Essential for Anaerobic growth of Escherichia coli on Xylose. J. Bacteriol. 186 (22), 7593–7600. https://doi.org/10.1128/JB.186.22.7593-7600.2004.
Horiuchi, J.I., Shimizu, T., Tada, K., Kanno, T., Kobayashi, M., 2002. Selective production of organic acids in anaerobic acid reactor by pH control. Bioresour. Technol. 82 (3), 209–213. https://doi.org/10.1016/S0960-8524(01)00195-X.
Hunter, C.N., Beatty, F.D., Thurnauer, M.C., Thomas, J., 2009. In: Hunter, C.N., Daldal, F., Thurnauer, M.C., Beatty, J.T. (Eds.), State Journal of Medicine. Springer Netherlands, New York. https://doi.org/10.1007/978-1-4020-8815-5 (Vol. 28, Issue 3).
Imam, S., Yilmaz, S., Sohmen, U., Gorzalski, A.S., Reed, J.L., Noguera, D.R., Donohue, T. J., 2011. IRsp1095: a genome-scale reconstruction of the Rhodobacter sphaeroides metabolic network. BMC Syst. Biol. 5 (July) https://doi.org/10.1186/1752-0509-5-116.
Inui, M., Momma, K., Matoba, R., Ikuta, M., Yamagata, H., Yukawa, H., 1995. Characterization of alcohol-assimilating photosynthetic purple non-sulfur bacteria and cloning of molecular chaperones from a purple non-sulfur bacterium. Energy Convers. Manag. 36 (6–9), 767–770. https://doi.org/10.1016/0196-8904(95)00117-V.
Jang, J.W., Jung, H.M., Im, D.K., Jung, M.Y., Oh, M.K., 2017. Pathway engineering of Enterobacter aerogenes to improve acetoin production by reducing by-products formation. Enzym. Microb. Technol. 106, 114–118. https://doi.org/10.1016/j.enzmictec.2017.07.009.
Johns, A.T., 1952. The Mechanism of Propionic Acid Formation by Clostridium propionicum. J. Gen. Microbiol. 6 (1–2), 123–127. https://doi.org/10.1099/00221287-6-1-2-123.
Khanna, N., Kumar, K., Todi, S., Das, D., 2012. Characteristics of cured and wild strains of Enterobacter cloacae IIT-BT 08 for the improvement of biohydrogen production. Int. J. Hydrog. Energy 37 (16), 11666–11676. https://doi.org/10.1016/j.ijhydene.2012.05.051.
Kleerebezem, R., Van Loosdrecht, M.C.M., 2007. Mixed culture biotechnology for bioenergy production. Current Opinion in Biotechnology 18 (3), 207–212. https://doi.org/10.1016/j.copbio.2007.05.001.
Kopf, S.H., Newman, D.K., 2012. Photomixotrophic growth of Rhodobacter capsulatus SB1003 on ferrous iron. Geobiology 10 (3), 216–222. https://doi.org/10.1111/j.1472-4669.2011.00313.x.
Kuenen, J.G., 2019. Continuous cultures (Chemostats). In: Reference Module in Biomedical Sciences. Elsevier, pp. 743–761. https://doi.org/10.1016/B978-0-12-801238-3.02490-9.
Lamed, R.J., Lobos, J.H., Su, T.M., 1988. Effects of stirring and hydrogen on fermentation products of Clostridium thermocellum. Appl. Environ. Microbiol. 54 (5).
Ling, J., de Toledo, R.A., Shim, H., 2016. Biodiesel production from wastewater using oleaginous yeast and microalgae. In: Environmental Materials and Waste: Resource Recovery and Pollution Prevention, pp. 179–212. https://doi.org/10.1016/B978-0-12-803837-6.00008-1.
Madigan, M., Cox, J.C., Gest, H., 1982. Photopigments in Rhodopseudomonas capsulata cells grown anaerobically in darkness. J. Bacteriol. 150 (3), 1422–1429. https://doi.org/10.1128/JB.150.3.1422-1429.1982.
Martens, D.E., Béal, C., Malakar, P., Zwietering, M.H., Van 'T Riet, K., 1999. Modelling the interactions between Lactobacillus curvatus and Enterobacter cloacae: I. Individual growth kinetics. International Journal of Food Microbiology 51 (1), 53–65. https://doi.org/10.1016/S0168-1605(99)00095-1.
NCBI, n.d. NCBI. (n.d.). Gene [Internet]. Bethesda (MD): National Library of Medicine (US), National Center for Biotechnology Information; 2004 – [cited YYYY Mmm DD]. Available from: https://www.ncbi.nlm.nih.gov/gene/No Title.
Oh, S.E., Logan, B.E., 2005. Hydrogen and electricity production from a food processing wastewater using fermentation and microbial fuel cell technologies. Water Res. 39 (19), 4673–4682. https://doi.org/10.1016/j.watres.2005.09.019.
Pearman, P.B., Guisan, A., Broennimann, O., Randin, C.F., 2008. Niche dynamics in space and time. Trends in Ecology and Evolution 23 (3), 149–158. https://doi.org/10.1016/j.tree.2007.11.005.
Pechter, K.B., Gallagher, L., Pyles, H., Manoil, C.S., Harwood, C.S., 2016. Essential genome of the metabolically versatile alphaproteobacterium Rhodopseudomonas palustris. J. Bacteriol. https://doi.org/10.1128/JB.00771-15.
Pfennig, N., 1977. Phototrophic green and purple bacteria: a comparative, systematic survey. In: Annual Review of Microbiology, 31, pp. 275–290. https://doi.org/10.1146/annurev.mi.31.100177.001423.
Puyol, D., Batstone, D.J., Hülsen, T., Astals, S., Peces, M., Krömer, J.O., 2017. Resource recovery from wastewater by biological technologies: Opportunities, challenges, and prospects. Front. Microbiol. 7, 1–23. https://doi.org/10.3389/fmicb.2016.02106.
Qin, C., Lei, Y., Wu, J., 2018. Light/dark cycle enhancement and energy consumption of tubular microalgal photobioreactors with discrete double inclined ribs. Bioresour. Bioprocess. 5 (1) https://doi.org/10.1186/s40643-018-0214-8.
Rai, P.K., Singh, S.P., 2016. Integrated dark- and photo-fermentation: Recent advances and provisions for improvement. International Journal of Hydrogen Energy 41 (44), 19957–19971. https://doi.org/10.1016/j.ijhydene.2016.08.084.
Rombouts, J.L., Mos, G., Weissbrodt, D.G., Kleerebezem, R., Van Loosdrecht, M.C.M., 2019a. Diversity and metabolism of xylose and glucose fermenting microbial communities in sequencing batch or continuous culturing. FEMS Microbiol. Ecol. 95 (2), 233. https://doi.org/10.1093/femsec/fiy233.
Rombouts, J.L., Mos, G., Weissbrodt, D.G., Kleerebezem, R., Van Loosdrecht, M.C.M., 2019b. The impact of mixtures of xylose and glucose on the microbial diversity and fermentative metabolism of sequencing-batch or continuous enrichment cultures. FEMS Microbiol. Ecol. 95, 112. https://doi.org/10.1093/femsec/fiz112.
Soto-Martin, E.C., Warnke, I., Farquharson, F.M., Christodoulou, M., Horgan, G., Derrien, M., Faurie, J.-M., Flint, H.J., Duncan, S.H., Louis, P., 2020. Vitamin Biosynthesis by Human Gut Butyrate-Producing Bacteria and Cross-Feeding in Synthetic Microbial Communities. https://doi.org/10.1128/mBio.00886-20.
Stomp, M., Huisman, J., Stal, L.J., Matthijs, H.C.P., 2007. Colorful niches of phototrophic microorganisms shaped by vibrations of the water molecule. ISME J. 1 (4), 271–282. https://doi.org/10.1038/ismej.2007.59.
Tanisho, S., 1998. Hydrogen production by facultative anaerobe Enterobacter aerogenes. In: Zaborsky, O.R., Benemann, J.R., Matsunaga, T., Miyake, J., San Pietro, A. (Eds.), BioHydrogen. Springer, US, pp. 273–279. https://doi.org/10.1007/978-0-585-35132-2_35.
Temudo, M.F., Muyzer, G., Kleerebezem, R., Van Loosdrecht, M.C.M., 2008. Diversity of microbial communities in open mixed culture fermentations: Impact of the pH and carbon source. Appl. Microbiol. Biotechnol. 80 (6), 1121–1130. https://doi.org/10.1007/s00253-008-1669-x.
Tsuji, A., Kaneko, Y., Takahashi, K., Ogawa, M., Goto, S., 1982. The Effects of Temperature and pH on the growth of eight Enteric and nine Glucose Non-Fermenting Species of Gram-negative Rods. Microbiol. Immunol. 26 (1), 15–24. https://doi.org/10.1111/j.1348-0421.1982.tb00149.x.
Venegas, D.P., De La Fuente, M.K., Landskron, G., González, M.J., Quera, R., Dijkstra, G., Harmsen, H.J.M., Faber, K.N., Hermoso, M.A., 2019. Short chain fatty acids (SCFAs) mediated gut epithelial and immune regulation and its relevance for inflammatory bowel diseases. Frontiers in Immunology 10 (MAR), 277. https://doi.org/10.3389/fimmu.2019.00277. Frontiers Media S.A.
Vos, P., Garrity, G., Jones, D., Krieg, N.R., Ludwig, W., Rainey, F.A., Schleifer, K.-H., Whitman, W.B., 2005. Bergey's Manual® of systematic bacteriology. In: Brenner, D. J., Krieg, N.R., Staley, J.T. (Eds.), Bergey's Manual® of Systematic Bacteriology. Springer, US. https://doi.org/10.1007/0-387-29298-5.
Wijffels, R.H., Barten, H., Reith, R.H., 2003. In: Reith, J.H., Wijffels, R.H. (Eds.), Bio-methane and Bio-hydrogen: Status and Perspectives of Biological Methane and Hydrogen Production. Dutch Biological Hydrogen Foundation.
Winkler, Boets, P., Hahne, B., Goethals, P., Volcke, E.I.P., Mari, K.H., 2017. Effect of the dilution rate on microbial competition: r-strategist can win over k-strategist at low substrate concentration. PLoS ONE 12 (3), e0172785. https://doi.org/10.1371/journal.pone.0172785.
Zagrodnik, R., Laniecki, M., 2016. An unexpected negative influence of light intensity on hydrogen production by dark fermentative bacteria Clostridium beijerinckii. Bioresour. Technol. 200, 1039–1043. https://doi.org/10.1016/j.biortech.2015.10.049.